9. Next morning the BF_3 is pumped out of the counter into trap 5, and the counter pumped down to a hard vacuum.

10 and 11. Same as items 5 and 6 high pressure schedule.

12 to 14. Same as items 10 to 12 high pressure schedule.

15. Argon is admitted to make up to the total pressure to 50 cm. After several hours to allow proper mixing of the gases, the counter is sealed off.

16. Same as item 14, high pressure schedule.

A gold foil is included in the pumping line to the counter to trap residual mercury vapor. Other than those mentioned in the schedule, no special precautions are taken except those compatible with good vacuum technique. Conventional stopcocks are used and all traps can be taken apart for cleaning. Taps and the trap ground joints are greased sparingly with Apiezon *L* or *M* grease.

The amount of complex required for a given filling is calculated and a little more than this quantity put in the flask. This allows the first and last fractions to be discarded, and since all the BF_3 is taken off each time, each filling is comparable.

THE REVIEW OF SCIENTIFIC INSTRUMENTS VOLUME 21, NUMBER 8 AUGUST, 1950

The Design of a Magnetic Focusing Coincidence Spectrometer*

C. M. FOWLER** AND R. G. SHREFFLER†
Randall Laboratory of Physics, University of Michigan, Ann Arbor, Michigan
(Received April 13, 1950)

Design and operating features are described for a semi-circular magnetic focusing coincidence spectrometer. The primary function of the spectrometer is that of determining whether or not two different radiations from a radioactive sample are in the same branch of the nuclear decay scheme. Although the instrument is designed primarily for studies between conversion electron groups, it is also suitable for studies between conversion groups and beta-spectra.

A feature of the instrument is its extraordinarily good coincidence resolving power. Applications of the spectrometer to two activities are briefly discussed, and an explanation of the high resolving power is given.

1. INTRODUCTION

THE primary function of the magnetic focusing coincidence spectrometer is to determine whether or not two different electron radiations of an active element are in cascade, that is, in the same branch of a decaying nucleus. The electrons may arise from the continuous beta-spectrum of an activity and from conversion electrons. Although no experimental data is offered for the case of photo-electrons, studies could include these as well.

The basic principle of the instrument involves the magnetic focusing of electrons from one of the radiations into one Geiger tube, while those of the other radiation are focused into a second Geiger tube. If the two radiations are in cascade, then a coincidence circuit collecting the inputs of the two Geiger tubes will record true coincidences. If no true coincidences are observed, the radiations are not in cascade.

FIG. 1. Fully assembled coincidence spectrometer.

For decay schemes exhibiting gamma-radiations which are moderately or strongly converted, the spectrometer offers a useful and certain method for properly ordering the radiations. The advantage of the spectrometer over the usual absorption coincidence techniques is that the radiations may be focused and studied in pairs through their conversion electrons, thus leaving no ambiguity as to which of several radiations may be in coincidence.

Feather,[1] as early as 1940, described a coincidence spectrometer designed primarily for coincidence studies between one conversion electron group and a beta-spectrum. Feather, Kyles, and Pringle[2] first reported the results of a specific investigation of this type in 1948.

The spectrometer described here is designed primarily to study coincidences between two conversion electron groups, and as will be shown later, exhibits very high coincidence resolving power. Among other details, it differs from that described by Feather, in that the coincidence radiations focused into the two Geiger tubes both travel through the same portion of the active source, and do not pass through the sample backing. This feature accounts in part for the high resolution of the spectrometer.

Limitations to which the spectrometer is subject

* Sponsored in part by ONR and the AEC (through NRC Predoctoral Fellowship Funds).

** Now at Kansas State College, Department of Physics, Manhattan, Kansas.

† Now at Los Alamos Scientific Laboratory, Los Alamos, New Mexico.

[1] N. Feather, Proc. Camb. Phil. Soc. **36**, 224 (1940).

[2] Feather, Kyles, Pringle, Proc. Phys. Soc. **61**, 466 (1948).

include: 1. Only radiations suitably converted may be studied. A rough rule (modified considerably for branched decay schemes) is that the product of the conversion coefficients of the radiations studied should not be appreciably less than 0.001. 2. Only conversion groups which can be focused two or more centimeters apart on the focal plane may be studied as a pair. This is a design limitation arising from the finite widths of the Geiger tubes. This restriction is usually only severe for high energy radiations (greater than 200 kev) or for elements of low atomic number. This is true, since for studies between gamma-radiations of nearly the same energy, by proper adjustment of the magnetic field, one Geiger tube may collect electrons from the K conversion group of one radiation, while the other tube may collect L conversion electrons from the other radiation. 3. Operational times required to build up adequate statistics are frequently quite long. This is an inherent difficulty brought about by large solid angle losses required for focusing. For activities of lifetimes less than a few days, the method becomes unfeasible unless the radiations are highly converted. 4. Two radiations delayed long with respect to the resolving time of the coincidence circuit will not yield appreciable true coincidences. It is therefore necessary to know from other investigations whether or not long delays are present in an activity before it can be assumed that two radiations are not in cascade, when they produce no true coincidences.

2. DESIGN DETAILS OF THE SPECTROMETER

Figure 1 is a photograph of the fully assembled coincidence spectrometer. The assembly consists of a camera, a vacuum system, a magnet, and a recording system. These components are described in the following sections:

The Camera

The design of the camera (scale drawing, Fig. 2) is based upon the principles incorporated in the photographic semi-circular spectrometer. Instead of a photographic plate, two movable Geiger tubes, controllable from outside the camera, open upon the focal plane.

The camera is constructed of $\frac{3}{8}$ in. brass plate. Bronze bolts seat the removable top on a rubber gasket, which in turn is contained in a channel milled around the top edges of the camera sides. When the camera is in proper position between the magnet pole faces, a flanged connection can be coupled to the vacuum line.

A rigid three-sided frame, supporting the sample, slit, and Geiger tube assemblies is mounted upon the camera floor, and secured by set screws. The sample and slit assemblies are shown in the plan view of Fig. 2 The slits are made of Lucite, and can be separated from 0 to 2 centimeters. Provisions are also made to allow variation of the separation of source and slit planes from one to five centimeters.

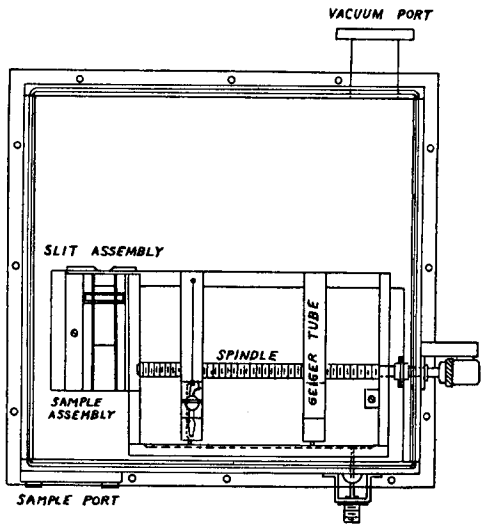

FIG. 2. Camera plan view; scale drawing.

The Geiger tubes are moved by threaded spindles, rotated by control knobs outside the camera. Veeder-Root counters, connected to the spindles, record the positions of the tubes. The control knob assembly can be separated from the drive spindles by uncoupling flanged connections, when it is necessary to remove the frame from the camera. The Geiger tubes receive their anode voltages through spring loaded contact pieces which make contact with copper bar conductors. These conductors are embedded in the Lucite rear wall of the frame. The spring loaded contacts are also mounted in Lucite pieces, which are bolted onto the ends of the Geiger tubes. Soldered to the copper conductor bars in the frame, are female sockets into which covar conductors slide, when the frame is properly placed within the camera. The covar conductors are permanently mounted on the camera, and lead through the camera walls to external amphenol fittings.

A $\frac{1}{32}$ in. celluloid lining, over all interior parts of the camera exposed to radiation, practically eliminates detectable scattering.

The Vacuum System

The vacuum system comprises two stages, a mechanical fore-pump, and a water-cooled, oil diffusion pump. Thermocouple vacuum plug units are installed in the system so that pressures within the camera, and between the two pumps can be read. A manometer, with a double stopcock arrangement, is incorporated into the system so that pressures may be built up slowly when the camera is opened. This procedure avoids undue strains on the Geiger tube windows.

Normal operating pressures of approximately one micron are used. These low pressures minimize electron air scattering and are more than sufficient to prevent the high anode voltages from breaking down within the camera.

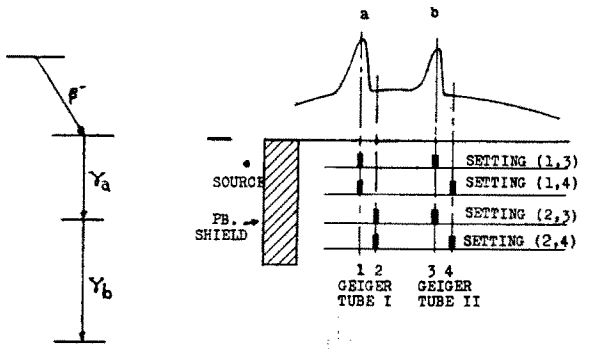

FIG. 3. Sketch illustrating offset method.

The Magnet

The chief property required of the magnet is stability. As will be shown later, the slightest drifting of the magnetic field greatly reduces the effectiveness of the instrument.

The stability required was obtained by butting a large number of Alnico No. 3 cylinders (1 in. $D \times 3$ in.) between the yoke and pole pieces. After establishing a convenient magnetic field, by pulsing current through fixed exciting coils, slight drifts up to one percent occur during the first few hours. After 24 hours, no further detectable changes are observed over periods of months.

By spacing the Alnico cylinders uniformly over the pole faces, except for a small increase in density near the face edges to help compensate for fringing flux, fields uniform out to nearly a half pole-gap width from the face edges may be obtained.

Recording System

Individual Geiger tube pulses are monitored by commercial IDL scalars. Pulses are then sent to a Rossi type coincidence circuit, including a pulse height selector discriminator circuit. Coincidences are recorded by a thyratron driven mechanical recorder. The time constant of the coincidence circuit can be varied by switching in various pairs of different valued grid leak resistors. By suitable choices of the RC constant of the Rossi circuit and pulse heights, the over-all circuit resolving time may be varied from 0.2 to 2 μsec.

For the Geiger tubes employed, drift time losses were found to be negligible for resolving times greater than 0.45 μsec.

3. ANALYSIS OF COINCIDENCE DATA

The procedure used in the study of two radiations sometimes varies, but the most useful one usually consists of fixing one Geiger tube at about the peak of one of the electron groups, while the other tube is set at various locations about the other line. A plot of the coincidence rates so obtained *versus* the position of the variable tube gives rise to the coincidence lines shown in Figs. 8, 9, and 10. The most noticeable feature of these lines is their sharpness, as compared to the lines seen when the instrument is operated as an ordinary non-coincidence spectrometer.

Studies to be published later will discuss the application of the spectrometer as a tool to resolve L_{I}, L_{II}, and L_{III} conversion electron groups in a more quantitative manner, as well as its use in distinguishing conversion lines arising from gamma-radiations of almost the same energies.

Observed coincidence rates consist of spurious coincidences and coincidences resulting from cascade radiations of the active isotope. Both require discussion.

Spurious Coincidences

There are two sources of spurious coincidences: accidentals and cosmic-ray coincidences.

Accidental coincidences are subtracted from all observed rates according to the well-known formula, $q_A = 2\tau n_1 n_2$, q_A being the accidental rate, τ the resolving time of the coincidence circuit, n_1 and n_2 the input counting rates entering the coincidence circuit.

Experimental studies showed that, to within the statistical accuracy of the research, hard components of cosmic radiation contributed a coincidence rate depending only upon the Geiger tube separations, the rate decreasing as the separation increases. From each observed coincidence rate, a cosmic-ray rate is thus deducted.

True Coincidences

When the spurious rates have been deducted from the observed rates, the resultant rates represent coincidences arising from nuclear cascade radiations. However, in addition to the coincidence rates sought between conversion electron groups, there exist smaller true coincidence rates between the conversion electrons focused in one Geiger tube, and portions of the continuous beta-spectrum focused in the other tube. Further, if the source shielding (see Fig. 3) is insufficient to absorb all of the lateral gamma-radiation, coincidences between the gamma-ray leakage and both conversion electrons groups and the continuous beta-spectrum will be present.

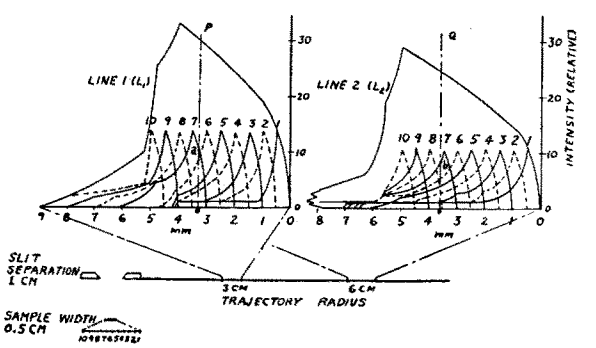

FIG. 4. Contributions of source increments to gross line densities. The number specifying the sample increment also identifies the contribution of this increment to the two gross lines.

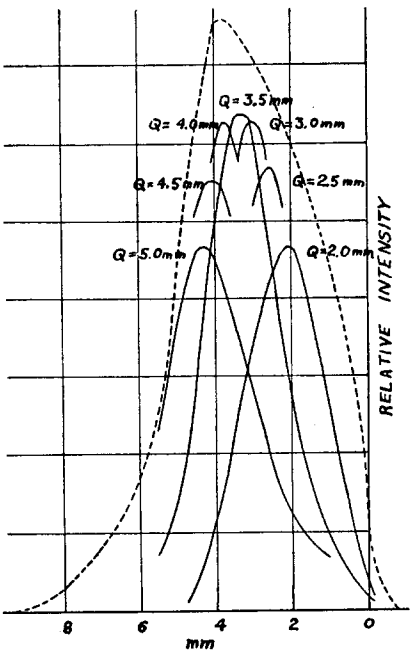

FIG. 5. Effect of fixed Geiger tube location on the shape and position of the coincidence lines. The values of Q given at the peaks of the curves locate the center of the fixed Geiger tube with respect to the leading edge of the gross density curve of line L_2. Geiger tube window widths: 1.5 mm.

The combined rates of all these cross coincidence terms may be eliminated by use of the "offset" method described below, leaving a net rate for the conversion electron coincidences alone.

In Fig. 3, let c_a and c_b represent conversion electron groups, between which coincidence studies are to be made. Suppose the positions 1 and 3 represent arbitrary points, one for each of the lines, at which the Geiger tubes are centered. Points 2 and 4 are offset points, such that the inner edges of the Geiger tube windows just clear the leading edges of the conversion lines. Then the true coincidence rate $Q(1,3)$ for the Geiger tubes centered at points 1 and 3 is given by the following equation:

$$Q(1,3)=q(1,3)-q(1,4)-q(2,3)+q(2,4). \qquad (1)$$

The small q's are the coincidence rates for the pairs of settings shown in Fig. 3. These rates are supposedly corrected for spurious coincidences.

Details of the proof for this formula, and its degree of validity are discussed in the Appendix.

4. COINCIDENCE LINE SHARPENING

The high coincidence resolution is a consequence of two effects, one arising from a minimization of source scattering of the electrons (an effect which accounts in considerable part for line broadening in non-coincidence spectrometry, particularly for lower energy radiations) and the other, a so-called natural line sharpening effect.

Both of these effects have as their common source the feature that a true coincidence can result only from electrons leaving the same atom of the source.

That the relatively intense scattered line portion seen in non-coincidence spectrometry is minimized here follows since both electrons forming a possible coincidence traverse about the same portion of the source; thus if one electron is scattered from the line peak, on the average, so would the other electron be scattered from its peak. Therefore unscattered electrons focused into one Geiger tube located at a line peak would be less likely to have highly scattered electrons in coincidence with them.

Aside from the reduction of line broadening due to source scattering, the following discussion shows that a natural line sharpening effect is also present. The arguments are given for a two-dimensional spectrometer and are thus only qualitative, but the important features entering into line sharpening are brought out clearly.

Suppose L_1 and L_2 are two conversion lines between which coincidence studies are to be made. The envelopes of the curves shown in Fig. 4 give the densities of the two lines. However, rather than the complete density curves, it is necessary to know the contribution of each element of the source to the density curve. In the discussion that follows, the complete line density curve will be referred to as the gross line, in distinction to the coincidence lines to be considered later. The integration of the gross line density curve over a Geiger tube window width, results in the lines as seen by either Geiger tube as it sweeps across the gross line.

Plotted below the gross density curves in Fig. 4 are shown the contributions to the curves from small elements of the source. The method of construction of these increment curves follows a treatment previously given by the authors.[3]

The total coincidence rate between a point P of line L_1 and a point Q of line L_2 is given by the sum of the coincidence rates furnished by each element of the

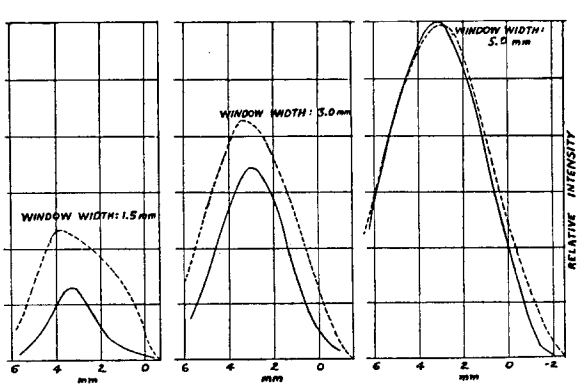

FIG. 6. Effect of Geiger tube window widths on shape of coincidence lines. Solid lines are coincidence lines; dotted lines show the corresponding integrated gross lines.

[3] Fowler, Shreffler, and Cork, Rev. Sci. Inst. **20**, 966 (1949).

source for these two points. For example, the coincidence rate between P and Q arising from the small source element 7, is given by the product $(oa)\cdot(ob)$. Contributions from all the source elements add to give the total coincidence rate for the pair of points P,Q.

In this manner, a rectangular grid can be drawn up giving the coincidence rates between any pair of points, one being taken from each of the two lines, L_1 and L_2.

The construction of these grids (one is necessary for each pair of gross lines to be studied) greatly facilitates the integrations over the Geiger tube window widths. In practice, it is found convenient to select equal spacings between the points P and Q, of the gross lines, such that an even number of these spacings are subtended by the Geiger tube windows. The total coincidence rate observed for specified locations of the two Geiger tubes will be comprised of the contributions from all pairs of points, P, Q, falling within the window widths covering portions of the gross lines. By use of conventional numerical integration formulas, the simultaneous integration over both Geiger tube window widths is readily accomplished, using the grid described above.

As mentioned previously, one of the procedures adopted in this research for coincidence studies, involves fixing one Geiger tube on one of the two lines, while the other tube is placed at various points of the other line. The distribution of coincidence rates plotted *versus* the movable tube setting gives rise to the sharp coincidence lines.

Theoretical coincidence lines following this procedure were then studied with gross line radii of 3.0 and 6.0 centimeters. The slit spacing was one centimeter, while a very wide source of 0.5 centimeter was used. The choice of this wide source was made to see if coincidence sharpening was still appreciable, and also to lend more accuracy to the numerical studies carried out, since the source could be conveniently divided into more increments.

Figure 5 shows the predicted coincidence lines, as the movable Geiger tube traverses the line L_1. The different curves arise from selecting different locations for the fixed Geiger tube on the line L_2. In this figure, both Geiger tube windows were taken as 1.5 mm wide.

Figure 6 shows the effect of Geiger tube window widths on the coincidence lines. For all these curves, the fixed Geiger tube was centered at the same point on line L_2. Since the gross line curves, integrated over different window widths are not the same, over each of the coincidence lines is plotted the window integrated gross line.

Some of the important observations from Fig. 5 are:

(1) The coincidence line intensities are strongly dependent upon the position of the fixed Geiger tube, being greatest when this tube is located on the leading edge of the gross line somewhat past its peak.

(2) The coincidence line widths are about half that of the integrated gross line width, thus showing coincidence sharpening. Even greater calculated sharpening should be expected with exact calculations replacing the triple numerical integrations.

(3) The locations of the peaks of the coincidence lines are also dependent upon the location of the fixed Geiger tube.

Some further observations from Fig. 6 are:

(4) The line sharpening improves as the window widths are decreased. For example, the ratio of half-widths of coincidence line to gross line decreased from 0.95 to 0.52 as the window widths changed from five mm to 1.5 mm.

(5) The coincidence line peak intensities increase with the window width.

5. APPLICATIONS OF THE SPECTROMETER

The Hafnium 181 Activity

For convenience of discussion of the coincidence studies, the decay scheme for this activity is given in Fig. 7.

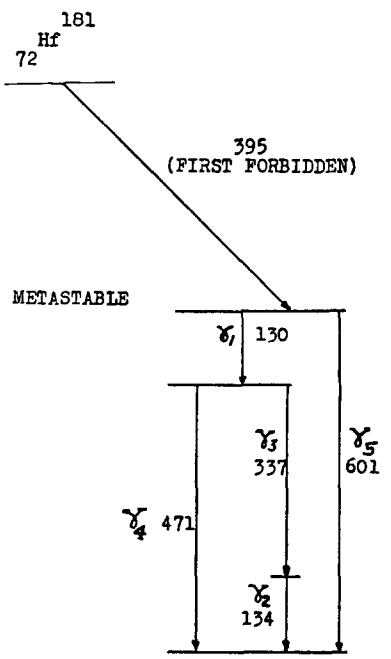

FIG. 7. Proposed decay scheme for Hf 181. All energies in kev.

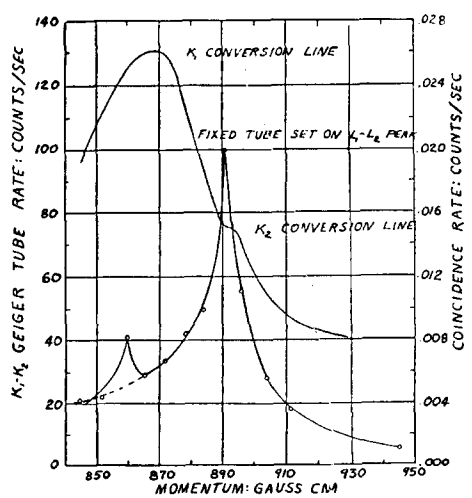

FIG. 8. Hafnium coincidence curve.

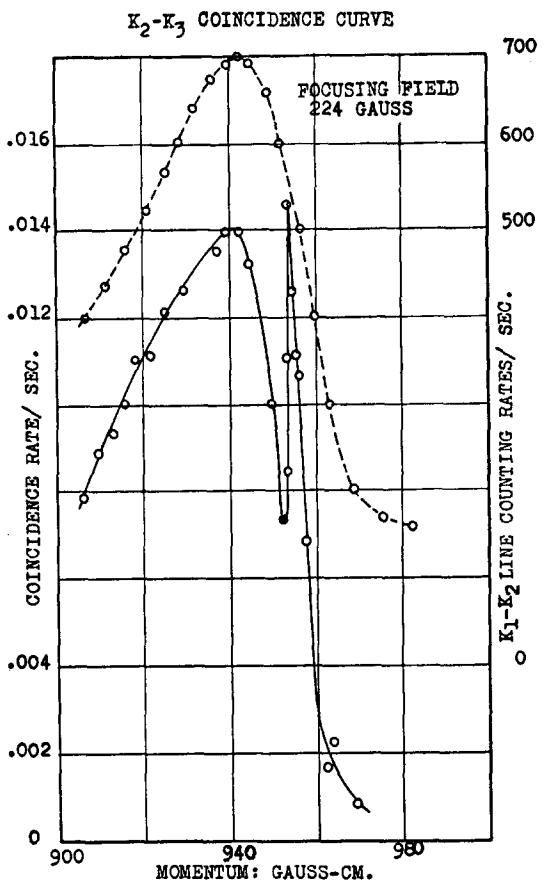

FIG. 9. Europium coincidence curve.

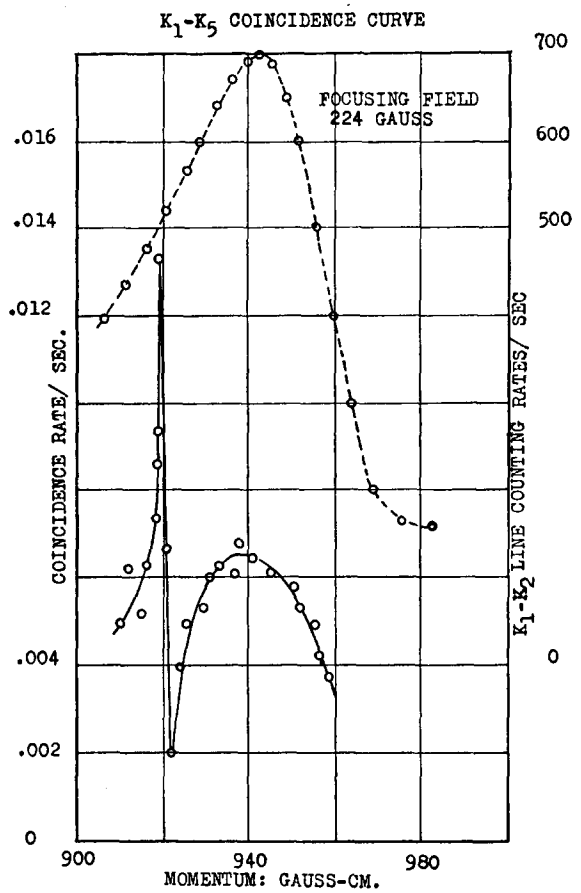

FIG. 10. Europium coincidence curve.

The initial report on the 48-day hafnium activity by Hevesy and Levi[4] has been followed by numerous papers. DeBenedetti and McGowan[5] first reported a metastable state of 22 microseconds following the initial beta-decay. Recently Chu[6] reported on the radiations from this element and proposed a decay scheme consistent with his analysis of the conversion and secondary spectra.

A preliminary survey of the conversion electron spectrum was undertaken by the authors in collaboration with E. Salmi. The results of this effort, with minor changes, agree with the report of Chu. The continuous beta-spectrum was found to be first forbidden with an end point of 395 kev; and a weak K conversion line corresponding to a gamma-energy of 601 kev was found with an intensity measured in units of the normalized beta-spectrum of approximately 0.0005. Chu reported the beta-spectrum to be allowed, and omitted the weak gamma-ray.

By making coincidence studies between various pairs of conversion electron groups, it was established that γ_1 is in coincidence with γ_2 and γ_3, and also that γ_2 and γ_3 are in coincidence, all in agreement with the decay scheme shown. Due to smaller coincidence intensities encountered it was difficult to show with statistical accuracy the anti-coincidence which should exist between conversion groups of γ_4 and either γ_2 or γ_3. No conversion line was found in coincidence with the continuous spectrum, establishing the previously reported position of the metastable state. Figure 8 shows a typical coincidence line. It records data confirming the coincidence between γ_1 and γ_2, and also illustrates the technique of employing the L conversion groups for radiations resulting from gamma-rays of nearly the same energies. Here, the fixed Geiger tube subtended portions of both L conversion groups, being centered at the peak of the unresolved L doublet.

Applications to the Long-Lived Europium Activities

When naturally occurring europium is subjected to thermal neutron bombardment, among others formed, are two long-lived activities (greater than five years) which exhibit a host of internal conversion lines.[7,8] Among these are two very intense lines of nearly the same energy: γ_1 (123 kev) and γ_2 (121 kev). Coincidence

[4] Hevesy and Levi, Kgl. Danske Vid. Sels., Math.-Fys. Medd. **15**, No. 11 (1938).
[5] DeBenedetti and McGowan, Phys. Rev. **74**, 728 (1948).
[6] K. Chu, Thesis (University of Michigan, 1949).
[7] Cork, Shreffler, and Fowler, Phys. Rev. **74**, 240 (1948).
[8] F. Shull, Phys. Rev. **74**, 917 (1948).

studies were made among these lines, and two of lesser intensity: γ_3 (244 kev) and γ_5 (344 kev).

Figures 9 and 10 show some of the results of these studies. In both figures the dotted lines show the unresolved K conversion lines of γ_1 and γ_2, as seen by a single Geiger tube. The solid curves show the coincidence lines obtained, as the inner Geiger tube is swept across the K doublet, while the outer Geiger tube is fixed under the K conversion line of γ_3 in Fig. 9, and under the K conversion line of γ_5 in Fig. 10. Although the cross coincidence terms have not been subtracted from the data of these figures, it is clear that γ_1 and γ_5 are in coincidence, as are γ_2 and γ_3.

As an example of the "offset" method, γ_3 and γ_5 were shown not to be in coincidence. Positions 1 and 3 correspond to the two line peaks, while 2 and 4 are points such that the inner edges of the Geiger tube windows just clear the conversion lines. The observed rates, corrected for spurious coincidences, were as follows:

$$q(1,3)=0.00345\pm0.00009 \text{ coinc/sec.}$$
$$q(1,4)=0.00353\pm0.00012 \text{ coinc/sec.}$$
$$q(2,3)=0.00283\pm0.00011 \text{ coinc/sec.}$$
$$q(2,4)=0.00285\pm0.00011 \text{ coinc/sec.}$$

From Eq. (1) this leaves as the net coincidence rate between K_3 and K_5:

$$Q(1,3)=-0.00006\pm0.00022 \text{ coinc/sec.}$$

This result is taken as evidence that γ_3 and γ_5 are not in coincidence.

With the coincidence data obtained supplementing other information known about these activities, it has been possible to propose plausible decay schemes for these activities, incorporating such features as K-capture, the presence of an isomeric state, three beta-spectra and numerous gamma-rays.[9]

Figures 9 and 10 together show the complete separation of the K conversion lines of γ_1 and γ_2. The remarkable coincidence resolution is evident upon noting that the radii of curvature of the conversion groups are only slightly greater than four centimeters.

ACKNOWLEDGMENTS

The authors are greatly indebted to Professor J. M. Cork for many valuable suggestions, as well as for continued encouragement. Acknowledgment is also due Dr. W. C. Parkinson of the University of Michigan Physics Staff for valuable discussions concerning the line sharpening effect. Finally, thanks are due to Professor E. K. Chapin of the Kansas State Physics Department and H. B. Keller of the University of Michigan, both of whom very kindly assisted the authors in the preparation of photographs.

[9] Cork, Keller, Rutledge, and Stoddard, Phys. Rev. **77** 848 (1950).

APPENDIX

Referring to the simple decay scheme of Fig. 3, it is seen that in the case of incomplete gamma-ray shielding, the Geiger tube counting rates are due not only to conversion electrons, but beta- and gamma-radiation as well. Thus for the setting (1,3), the total counting rates for the two tubes may be written as:

$$n_1=n_{1c_a}+n_{1\beta}+n_{1\gamma}$$

and

$$n_3=n_{3c_b}+n_{3\beta}+n_{3\gamma}.$$

The terms on the right represent partial rates from the conversion electrons, continuous beta-spectrum and gamma-ray leakage, respectively. The numerical subscripts refer to the positions of the Geiger tubes.

In addition to the coincidence rate between conversion electrons, which will involve the factor $n_{1c_a}n_{2c_b}$, cross coincidences between various combinations of the partial counting rates will occur, for example between the pairs $(n_{1c_a},n_{3\beta})$ and $(n_{1\beta},n_{3\gamma})$.

To indicate the proof of Eq. (1), the partial coincidence rate due to the cross term n_{1c_a} and $n_{3\beta}$ will be computed. Let ω_1 be the fraction of conversion electrons of group c_a collected by Geiger tube I at setting 1, and ω_3 the fraction of the continuous beta-spectrum collected by Geiger tube II at setting 3. Let N be the total source strength. Then for each particle collected by tube II, there will be ω_1 coincidences with the converted electrons focused in tube I. Since there are $N\omega_3$ beta-particles collected per second in tube II, the partial coincidence rate may be written:

$$q(1c_a,3\beta)=N\omega_3\omega_1=n_{1c_a}n_{3\beta}/N.$$

The contributions of all other coincidence terms for each of the settings of Fig. 3 may be computed in similar fashion.

If it is now assumed that the small offsets of the Geiger tubes shown in Fig. 3 do not change the partial rates due to the beta-spectrum and gamma-ray leakage, we can write:

$$n_{1\beta}=n_{2\beta} \quad n_{1\gamma}=n_{2\gamma} \quad n_{3\beta}=n_{4\beta} \quad n_{3\gamma}=n_{4\gamma} \tag{A.1}$$

Using these approximations, and substituting all of the cross term coincidence rates, as computed above, for the various settings of Eq. (1), the net result becomes:

$$Q(1,3)=n_{1c_a}n_{3c_b}/N. \tag{A.2}$$

The offset procedure then eliminates all coincidence combinations except that between the conversion electrons.

The method of proof may be generalized to cover more complex decay schemes, taking account of branching, Geiger tube efficiencies etc., but in all cases, the offset method leaves only the rate arising from conversion electrons.

The assumptions involved in Eq. (A.1) are ordinarily quite good, since most beta-spectra are quite flat over the narrow regions subtended by conversion lines. In all cases, if necessary, a correction factor, based upon the shape of the beta-spectrum can be applied to the observed offset rates, if the offsets are quite large as may be required in case several closely spaced lines must be skipped before arriving to a line free portion of the beta-spectrum. Measurements of gamma-ray leakage have shown that over the narrow offsets employed, the decrease in intensities are scarcely detectable.

Finally it should be remarked that, although the offset procedure correctly leaves only the coincidence rates between conversion electrons, the final formulas given by the above proof, such as Eq. (A.2) have failed to take into account the line sharpening effect existing between the conversion groups. Implicitly assumed in the above proof, was the uniformity of coincidence rates between the various cross terms over all increments of the Geiger tube windows. This assumption is essentially correct for all the combinations except that where both of the terms are from conversion lines. Here, the sharpening effect must be considered for an accurate calculation of this coincidence rate.